CHARACTERIZATION AND PROVENANCE OF LIME PLASTERS FROM THE TEMPLO MAYOR OF TENOCHTITLAN (MEXICO CITY)*

D. MIRIELLO,† D. BARCA and G. M. CRISCI

Dipartimento di Scienze della Terra, Università degli Studi della Calabria, via Pietro Bucci, 87036 Arcavacata di Rende (CS), Italy

L. BARBA, J. BLANCAS and A. ORTÍZ

Instituto de Investigaciones Antropológicas, Universidad Nacional Autónoma de México, Ciudad Universitaria 3000, Delegación Coyoacán 04360 D.F.

A. PECCI

ERAAUB, Facultat de Geografia i Història, Universitat de Barcelona, Montalegre 6-8, 08001 Barcelona, Spain

and L. LÓPEZ LUJÁN

Museo Templo Mayor, Instituto Nacional de Antropología e Historia (INAH), Guatemala 60, Centro 06060 México, D.F.

In this work, we present the results of the analyses of 20 lime plaster samples taken from the Templo Mayor (Great Temple), the main pyramid of Tenochtitlan (Mexico), the ancient capital of the Mexicas. The samples were analysed to recover information on the mixtures used in the fabrication of the plasters and for the provenance of the raw materials (in particular, limestone) used to make the plasters. The characterization of the samples was done by OM, SEM/EDS, XRF and LA–ICP–MS analyses, while the identification of the provenance of raw materials was done by studying the lumps present in the samples with LA–ICP–MS. The objective of the study was to establish if there was a relationship between changes in the construction techniques employed in the pyramid over time and if there were changes in the provenance of the raw materials. Six different construction phases of this pyramid are analysed, showing the similarities and differences among them, mainly based on differences in the sieving of the aggregates and in the raw materials employed. The provenance studies of the limestone used to make the plasters demonstrated that all the limestone comes from the Tula region.

KEYWORDS: LIMESTONE, LUMP, PROVENANCE, OM, XRF, SEM–EDS, ICP–MS LASER ABLATION, LIME PLASTER, MORTAR, CONSTRUCTION PHASES, TEZONTLE, TEMPLO MAYOR

INTRODUCTION

Detailed studies of ancient artificial products have helped to solve important historical, archaeological and technological problems, including the provenance of the raw materials and their manufacture (Franzini *et al.* 2000; Moropoulou *et al.* 2000; Damiani *et al.* 2003; Crisci *et al.*

2004; Meir *et al*. 2005; Miriello and Crisci 2006; Barba *et al*. 2009; Miriello *et al*. 2010a,b; Ruffolo *et al*. 2010; Scarpelli *et al*. 2010; Miriello *et al*. 2011). The application of the characterization studies to the plasters has also helped in the identification of different construction phases in the archaeological and historical buildings (Vendrell-Saz *et al*. 1996; Crisci *et al*. 2001, 2002; Moropoulou *et al*. 2003; Carò *et al*. 2008; Miriello *et al*. 2010c).

In this work, we present the results of the analyses of 20 lime plaster samples taken from six construction phases of the Templo Mayor (Great Temple), the main pyramid of Tenochtitlan (Mexico), the ancient capital of the Mexicas. As with most of the Mesoamerican religious buildings, the Templo Mayor—first erected in AD 1325 and destroyed by the Spaniards in AD 1521–1522—is composed of different construction phases that were built through time one on top of the other, taking advantage of the volume of the former phases. The Templo Mayor was totally rebuilt seven times, enlarging its four façades; and it was partially remodelled six more times, enlarging just its western or northern façade (López Austin and López Luján 2009). The dating of these construction phases is under discussion (Table 1), although the second one should start at some time during the reign of Acamapichtli (AD 1375–1395) and phase VII should correspond to the reign of Motecuhzoma II (AD 1502–1529) (Matos Moctezuma 1981; Graulich 1987; Umberger 1987; López Luján 1993, 2006; López Austin and López Luján 2009).

The sampling of the plasters took into account all the different phases, from the second onwards. Unfortunately, the first one was not excavated after being detected and nowadays it is not possible to sample it. The samples were analysed to recover information on the mixtures used in the fabrication of the plasters and for the provenance of the raw materials (in particular, limestone) used to make the plasters. The aim of this study was to document whether there were similarities or differences among the consecutive construction phases, which could be related to political, economic or social changes in the Mexica society; or between samples of the same

Table 1   *The dating of the different phases of the main pyramid of Templo Mayor, following Matos (1981) and Umberger (1987) (López Luján 2006)*

Phase	Matos (1981)	Umberger (1987)
II	AD 1375–1427	
IIc	Acamapichtli	
	Huitzilihuitl	
	Chimalpopoca	
III	AD 1427–1440	
	Itzcoatl	
IV	AD 1440–1469	AD 1440–1469
IV A	Motecuhzoma I	Motecuhzoma I
IV B	AD 1469–1481	
	Axayacatl	
V	AD 1481–1486	AD 1469–1481
	Tizoc	Axayacatl
VI	AD 1486–1502	AD 1481–1502
	Ahuitzotl	Tizoc
		Ahuitzotl
VII	AD 1502–1520	
	Motecuhzoma II	

construction phases, which could reflect different origins of raw materials and/or different workers who could have taken part in the building process, whose technical choices were distinct from one another. These differences could have been revealed either by changes in the recipes used to prepare the plasters (relative proportions or the kind of raw materials employed) or by a different provenance of the raw materials. One of the possible differences that the archaeometrical study could verify is that suggested by Friar Diego Durán (1984: see also Nicholson 1987; López Luján *et al.* 2003; López Luján 2006), who reports that King Motecuhzoma I ordered a new enlargement of the Templo Mayor around AD 1467. The neighbouring cities would bring stone and would contribute to the building of each one of the façades: Texcoco that of the west, Chalco that of the south, Tlacopan that of the east and Xochimilco that of the north. The people from the Toluca Valley would bring supplies of sand, while those from the Cuernavaca area (in the modern state of Morelos) would provide the lime.

Regarding the provenance of the raw materials, in this work we focus in the limestone, being an important construction material that was not present in the immediate surroundings of Tenochtitlan. In fact, this was an island city, located in the middle of a volcanic basin, and the nearest geological limestone outcrops were located far away. According to the historical sources written during the 16th century, the Aztecs imported by way of tribute and commerce lime and limestone from different regions. For instance, the tributary lists known as the *Matrícula de Tributos* (1991, 22) and the *Codex Mendoza* (1992, 28r, 42r) record that lime loads were brought periodically from Tepeacac (a province located in the modern state of Puebla) and from Atotonilco de Pedraza (a province located on the northern border of the state of Mexico and the southwestern border of the state of Hidalgo). On the other hand, the native informants of Friar Bernardino de Sahagún (1979, xi:221r) speak about different kinds of limestone used to paint: *chimaltizatl* and *tetizatl*. After Sahagún (2000, 1132), the first came from Huaxtepec (near Cuernavaca, Morelos) and was sold in the market, while the second one was obtained 'in the small rivers near Tula' (in the modern state of Hidalgo). For the new enlargement of the Templo Mayor ordered around AD 1467 by Motecuhzoma I, mentioned above, the lime would have been provided by the people from the Cuernavaca area, in the modern state of Morelos (Durán 1984; Nicholson 1987; López Luján *et al.* 2003; López Luján 2006). Understanding the provenance of the limestone used in the plasters of Templo Mayor, and clarifying whether there were changes over time in the outcrops exploited, could therefore help in better understanding the relationship between the Mexicas and their neighbours in Central Mexico and verifying what the historical sources suggest.

The three areas in which the main outcrops were possibly exploited in Prehispanic times, located in the modern states of Morelos, Puebla and Hidalgo, have already been characterized in previous work done by our group that aimed at identifying the precedence of the limestone used in the fabrication of the plasters of the floors of the Teopancazco quarter centre at Teotihuacan (Barba *et al.* 2009). The two cities (Teotihuacan and Tenochtitlan) were in fact both located in the Basin of Mexico and had access to the same outcrops. Analyses were done by OM, SEM/EDS, XRF and LA–ICP–MS for the characterization of the samples, to establish whether there were differences within and between the construction phases, and to determine the raw materials used.

In order to establish the provenance of the limestone used in Templo Mayor, we have compared the results of the analyses of the lumps present in the Templo Mayor plasters to those obtained from the different outcrops. This methodology is based on the compositional similarities between the lumps (Bakolas *et al.* 1995) and the limestone used to produce the lime for plasters, and was successfully applied to establish the provenance of the limestone used to produce the plastered floors of the central patio of Teopanzaco (Teotihuacan) (Barba *et al.* 2009).

For the Templo Mayor samples, the lumps were also analysed using LA–ICP–MS.

The sampling was done taking into account the construction phases identified during the archaeological excavations. As said above, the construction phases from II to VII were sampled (Table 2 and Fig. 1). In this work, we call plasters the superficial layers rich in lime that were applied to cover all the different architectural elements (floors, walls, staircases) of the Templo Mayor. In these plasters, two layers are evident: a thin surface layer made of lime and with no aggregate, called 'enlucido'; and, below this, a layer with lime and aggregate. To distinguish the lower layer with aggregate from the 'enlucido', in the text it is called 'firme'. The presence of these layers in the samples coming from Templo Mayor can be observed at the macroscopic scale. Nevertheless, it can be better observed in the flatbed scanner images of thin sections under crossed polars (Fig. 2). In particular, samples TM2, TM6, TM7, TM8, TM9, TM10, TM11, TM13, TM15 and TM16 are composed of 'enlucido' and 'firme'. The 'enlucido' is only made of lime and its thickness varies from approximately 1 to 5.4 mm (Figs 2 (a) and 2 (b)). Beneath this layer there is the so-called 'firme'. This is a thicker layer composed of a microcrystalline calcitic binder and an aggregate that can be observed in the optical microscope.

Some of the samples coming from Templo Mayor were only of 'enlucido' (samples TM12 and TM18; Fig. 2 (c)). In some cases, this 'enlucido' is composed of several superimposed layers, a typical pattern in Mesoamerica. Other samples are only made of 'firme', possibly because the 'enlucido' was lost (samples TM1, TM3, TM4, TM5, TM14 and TM19; Fig. 2 (d)).

Table 2 *Samples taken from the different construction phases of Templo Mayor*

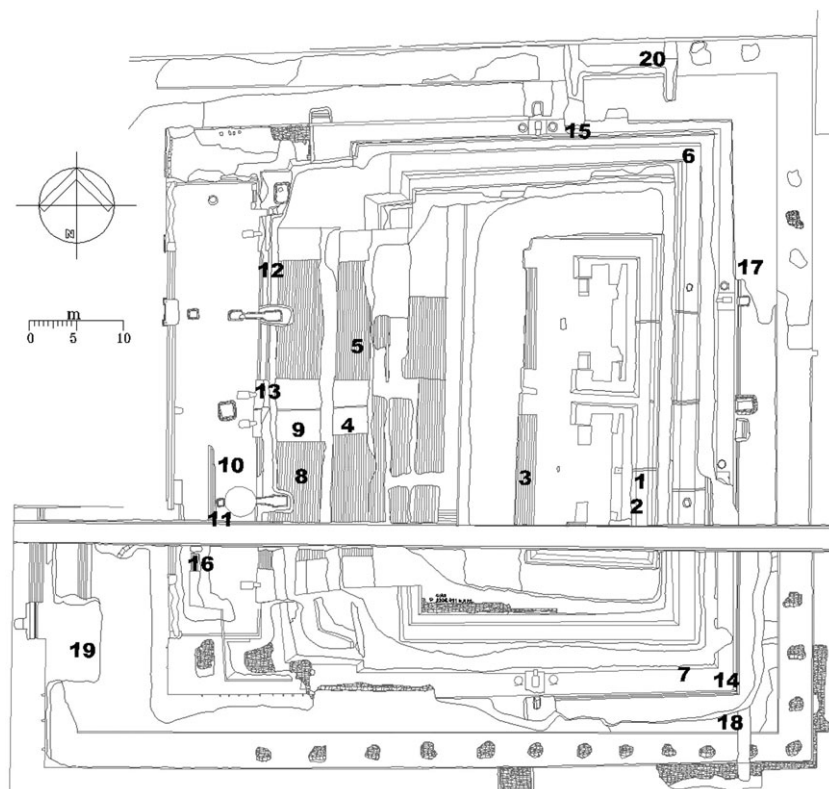| Sample	Construction phase	Sampling point
TM1	II	Floor
TM2	II	Wall
TM3	II	Staircase
TM4	III	Balustrade
TM5	III	Staircase
TM6	III	Floor
TM7	IV	Wall
TM8	IV	Wall
TM9	IV	Balustrade
TM10	IV A	Floor
TM11	IV A	Staircase
TM12	IV B	Staircase
TM13	IV B	Balustrade
TM14	IV B	Floor
TM15	V	Wall
TM16	V	Staircase
TM17	V	Floor
TM18	VI	Wall
TM19	VI	Platform floor
TM20	VII	Platform floor

Figure 1   *The archaeological plan of the Tenochtitlan's Templo Mayor, showing the location of the plaster samples.*

Finally, samples TM17 and TM20 are integrated by two layers of '*firme*' with different petrographic characteristics (Fig. 2 (e)). For this study, the different layers of the two samples were considered separately, and were numbered as samples TM17_I, TM17_II, and TM20_I, TM20_II. The samples labelled 'I' correspond to the upper layer, the last one to be applied, while those labelled 'II' correspond to the inner layer. For this study, the petrographic characterization was performed only on the '*firme*'.

ANALYTICAL TECHNIQUES

All the samples were examined in thin section, using transmitted polarized optical microscopy (OM) by means of a Zeiss microscope. For samples TM12 and TM18, it was not possible to study the aggregates, because they only consist of pure lime. The samples were studied on the polished plane surface by flatbed scanner images under reflected light. Glasses in volcanic rocks and lumps (Bakolas *et al*. 1995) of the aggregate were also analysed on polished thin sections, to determine the major chemical composition, by SEM–EDS microanalysis on an FEI Quanta 200 instrument, equipped with an EDAX Si (sapphire Li detector). The analysis of trace elements (^{45}Sc, ^{51}V, ^{53}Cr, ^{59}Co, ^{60}Ni, ^{66}Zn, ^{85}Rb, ^{88}Sr, ^{89}Y, ^{90}Zr, ^{93}Nb, ^{137}Ba ^{139}La, ^{140}Ce, ^{141}Pr, ^{208}Pb and ^{238}U) in the lumps was performed by laser ablation – inductively coupled plasma – mass spectrometry (LA–ICP–MS). The analyses were carried out at the Department of Earth Sciences, Università
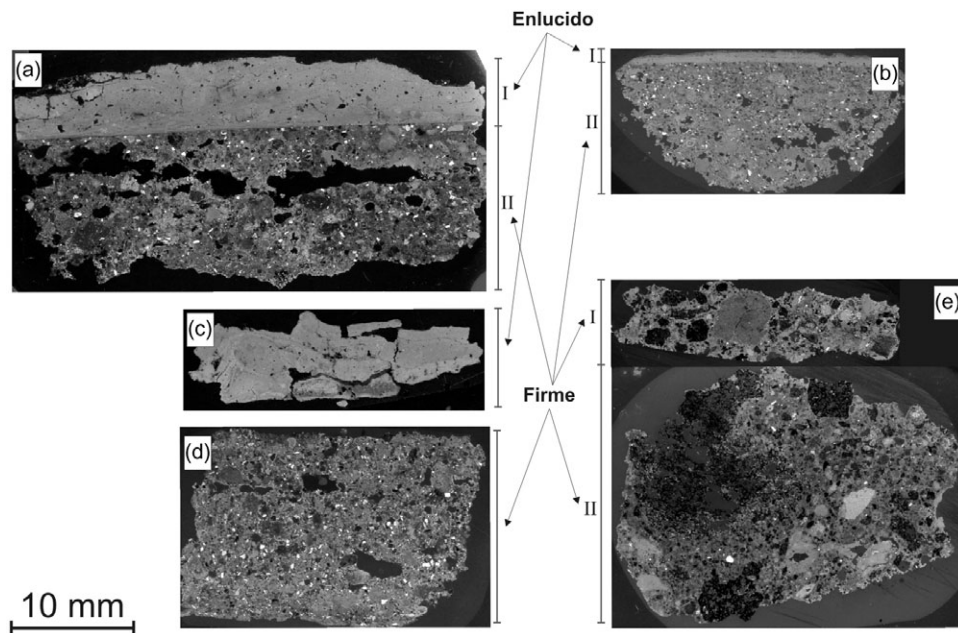
Figure 2   *Flatbed scanner images of plasters under crossed polars: (a) sample TM15, (b) sample TM2, (c) sample TM18, (d) sample TM4 and (e) sample TM20.*

della Calabria (Italy), using an Elan DRCe (PerkinElmer/SCIEX), connected to a New Wave UP213 solid state Nd–YAG laser probe (213 nm). Measurements were made on a section of 80–100 μm thickness. Samples were ablated by a laser beam in a cell, following the method tested by Gunther and Heinrich (1999). For each analysis, background levels for all elements were established by acquiring data for about 60 s (acquisition of gas blanks) before starting the 60 s of ablation. The data were transmitted to a PC and processed by the GLITTER program, which is a data reduction software program for the laser ablation microprobe, developed by the ARC National Key Centre for Geochemical Evolution and Metallogeny of Continents (GEMOC) at the Department of Earth and Planetary Sciences of Macquarie University. The calibration was performed using NIST glass reference materials: SRM612 (50 ppm being the nominal concentrations of the trace elements) and SRM610 (500 ppm being the nominal concentrations of the trace elements) (Pearce *et al*. 1997), in conjunction with internal standardization applying CaO concentrations (Fryer *et al*. 1995) from SEM–EDS analyses. The recent study by Wyndham *et al*. (2004) demonstrated that the use of a matrix-matching external standard is not essential, and that accurate and reproducible results can be obtained from different matrices using the NIST suite of glass standards (SRM610, SRM612 and SRM614), especially by using UV laser (Fallon *et al*. 2002; Lazareth *et al*. 2003; Sinclair 2005). Nevertheless, in order to evaluate possible errors, within each analytical sequence, determinations were also made on a pressed powder tablet using NIST standard SRM1d Argillaceous Limestone, analysed as an unknown sample, and compared with reference values certified by NIST for V, Ni, Rb, Sr, Y, Nb, La, Ce, Pr and U. For these elements, the accuracy, as the relative difference from reference values, was always better than 10%, and most elements plotted in the range ±5%. For Sc, Co, Cr, Zn and Zr, in the absence of NIST certification in the SRM1d standard, we used BCR2 standard glass from the USGS, obtaining the same accuracy (Barca *et al*. 2007).

To determine the provenance of the limestone used in the preparation of lime, we used the methodology developed in a previous paper by Barba *et al.* (2009), which is based on the compositional similarity of lumps with the probable provenance limestone quarries. The results of the analyses of the lumps were compared to those of the limestone of the possible outcrops that were exploited in the vicinity the Basin of Mexico, located in the surrounding areas of Tula, Puebla and Cuernavaca, that had already been studied (Barba *et al.* 2009).

<div align="center">RESULTS AND DISCUSSION</div>

Macroscopic description of the plasters

From a macroscopic point of view, it is possible to divide the plasters into different typologies. There is a main typological group that includes all of them, except for samples TM14, TM19 and TM20_II. The plasters belonging to this group have a brownish colour and a very coarse sand aspect (Wentworth 1922). The degree of cohesion is good. The plasters can, in fact, be broken only with a strong pressure of the fingers. The plasters show a good degree of preservation. An example of this group can be observed in Figure 3 (a).

There is a second small group that includes samples TM19 and TM20_II, in which it is possible to observe macroscopically the presence of volcanic cinders, which have a colour that goes from light red to dark red (Fig. 3 (c)). In Mexico, these cinders are called '*tezontle*', and they will be treated in greater depth later.

Finally, there is a sample which fits neither category, sample TM14 (Fig. 3 (b)). It is characterized by the presence of reused plaster fragments in the binder, which appear as clasts of dimensions that can reach centimetre sizes. Also in this sample, the cohesion is very good.

In the first group and in sample TM14, although the volcanic cinders cannot be seen macroscopically, it is sometimes possible to observe them in thin section under the microscope.
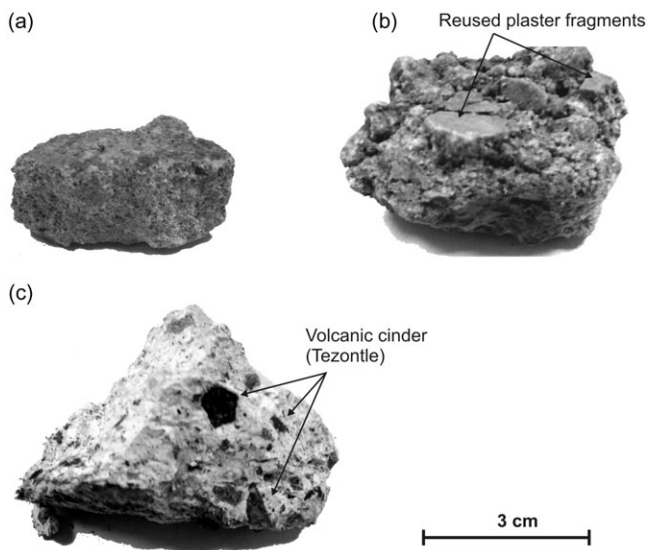

Figure 3   *Macrophotographs of (a) sample TM1, (b) sample TM14 and (c) sample TM19.*

Microscopic description of the plasters

The microscopic analysis in thin section allows us to reach a better level of detail in the study of the samples. The three groups of plasters examined in the macroscopic analyses show major complexity when observed with the polarized optical microscopy. As stated in the sampling, most samples are composed of an '*enlucido*' and a '*firme*', and a few other samples only of one of these layers. This can also be observed in the flatbed scanner images of the thin sections (Fig. 2). In general, the fragments forming the aggregate of the plasters have sizes between approximately 0.14 and 3.33 mm (Table 3). Most of the clasts have a high angularity and a good degree of sorting. Some samples (TM1, TM2, TM3, TM4, TM6, TM9, TM20_I and TM20_II; Table 3) contain traces of volcanic glass shards (Fig. 4 (a)). In many of them, it is possible to identify the presence of porphyric rhyolites (Fig. 4 (b)). Sometimes, fragments of pumice can also be recognized (Table 3). These fragments are very different in size and can vary from few microns to some millimetres (Fig. 4 (c) and Fig. 5 (d)). In most samples (except TM1, TM2, TM3 and TM4), fragments of volcanic cinder can be recognized. Their composition varies from that of basaltic trachyandesites to that of trachydacites, as is discussed later.

Apart from TM4, in the remaining samples it was possible to identify some lumps (Fig. 4 (f)) (Bakolas *et al*. 1995). Their presence, as shown in a previous work (Barba et al. 2009), is important to identify the provenance of the limestone used. Minerals included in the aggregate of all the samples are plagioclase (Fig. 5 (b)), amphibole (Fig. 5 (a)), opaque minerals and quartz (Fig. 5 (c)). In the samples that contain fragments of basaltic trachyandesites and trachydacites (Table 3), there are also traces of olivine (Fig. 4 (e)). The detailed petrographic composition of the different samples is summarized in Table 3. In sample TM3, there are traces of charcoal, due to the burning of vegetal material during the lime production process (Fig. 5 (f)). This charcoal was studied in order to identify the kind of wood employed in this activity.

Composition of the volcanic fragments

As stated above, the majority of the samples contain fragments of volcanic cinder, locally known as '*tezontle*'. These fragments can be recognized for their vesicular structure in thin section (Figs 4 (d) and 4 (e)), and because they show a variable colour that goes from dark grey to red under reflected light. The SEM–EDS analyses (Table 4) of volcanic fragments were classified by TAS diagram (Le Maitre *et al*. 2005). The results have shown that the red cinders have a composition that varies from the basaltic trachyandesites to that of the trachyandesites (Fig. 6). The dark grey cinders have a broader composition that varies from the basaltic trachyandesites to the dacites (Fig. 6). The red cinders were identified only in samples TM7, TM10, TM14, TM19 and TM20, which belong to construction phase IV and onwards. Except in sample TM19, where red cinder has been identified, it is always present in significant quantities, which makes it clear that it was added intentionally to the mixture. In these samples, the red cinder also shows a very high degree of sorting.

In contrast to the red cinders, the grey cinders are not well sorted. Furthermore, from the quantitative point of view, they can be found only in traces in the aggregate. It is then possible that they were not intentionally added to the mixture, but naturally present in the pyroclastic deposits used to obtain inert material for the mixtures. Probably, the types of '*tezontle*' used in the mixtures, and the outcrops from which they were brought to Tenochtitlan, are different. A detailed study on its provenance is currently in progress. The other volcanic fragments, the shards and the pumices have compositions compatible with those of porphyric rhyolites (Fig. 6).

Table 3   *Petrographic features on thin sections of plasters; the description refers to the 'firme' layers*

| | 'Enlucido' | By optical microscopy | | | | | | By optical microscopy and SEM–EDS analysis | | | | | |
		Max. aggregate size (mm)	Mean aggregate size (mm)	Max. macropores size (mm)	Angularity	Sorting	Mineralogical phases of the aggregate	Reused mortar fragments	Rhyolitic shard	Pumice	Porphyric rhyolite	Red (under reflected light) volcanic cinder ('tezontle')	Dark grey (under reflected light) volcanic cinder
TM1	A	0.81	0.33	1.38	H	H	Pl, Amp, Om, Qtz	A	P	P	P	A	A
TM2	P	1.68	0.31	2.90	H	H	Pl, Amp, Om, Qtz	A	P	P	P	A	A
TM3	A	0.50	0.14	5.30	H	M	Pl, Amp, Om, Qtz	A	P	P	P	A	A
TM4	A	1.55	0.35	4.25	H	M	Pl, Amp, Om, Qtz	A	P	A	P	A	A
TM5	A	4.17	0.39	1.52	H	M	Pl, Amp, Om, Qtz	A	A	A	P	A	A
TM6	P	7.71	0.50	6.27	H	M	Pl, Amp, Om, Ol, Qtz	A	P	P	P	A	Trachyandesite
TM7	P	2.16	0.57	0.46	H	M	Pl, Amp, Om, Ol, Qtz	A	A	P	P	Basaltic trachyandesite	A
TM8	P	2.00	0.46	2.41	H	M	Pl, Amp, Om, Ol, Qtz	A	A	P	P	A	Trachyandesite
TM9	P	4.90	0.37	6.37	H	L	Pl, Amp, Om, Ol, Qtz	A	P	P	P	A	Trachyandesite
TM10	P	2.27	0.63	1.49	H	M	Pl, Amp, Om, Ol, Qtz	A	A	P	P	Basaltic trachyandesite	A
TM11	P	0.68	0.23	1.06	H	M	Pl, Amp, Om, Qtz	A	A	A	A	A	Dacite
TM13	P	7.77	0.78	3.37	H	L	Pl, Amp, Om, Qtz	A	A	A	P	A	A
TM14	A	7.34	3.20	3.67	H	L	Pl, Amp, Om, Ol, Qtz	P	A	P	P	Basaltic trachyandesite	A
TM15	P	2.62	0.61	10.00	H	M	Pl, Amp, Om, Ol, Qtz	A	A	P	A	A	Basaltic trachyandesite; trachydacite andesite
TM16	P	1.59	0.41	2.84	H	M	Pl, Amp, Om, Ol, Qtz	A	A	A	A	A	Trachyandesite
TM17_I	A	0.40	0.28	0.35	H	M	Pl, Amp, Om, Ol, Qtz	A	A	A	A	A	Trachyandesite
TM17_II	A	0.61	0.31	0.75	H	M	Pl, Amp, Om, Qtz	A	A	A	P	A	A
TM19	A	3.37	0.59	1.93	M	L	Pl, Amp, Om, Ol, Qtz	A	A	A	A	Basaltic trachyandesite; trachyandesite	A
TM20_I	A	3.86	0.83	0.64	M	M	Pl, Amp, Om, Ol, Qtz	A	P	A	A	Trachyandesite	Trachyandesite
TM20_II	A	13.66	3.33	1.83	M	L	Pl, Amp, Om, Ol, Qtz	A	P	A	A	Basaltic trachyandesite; trachyandesite	A

Abbreviations: Amp, amphibole; Ol, olivine; Om, opaque minerals; Pl, plagioclase; Qtz, quartz; L, low; M, medium; H, high; A, absent; P, present.
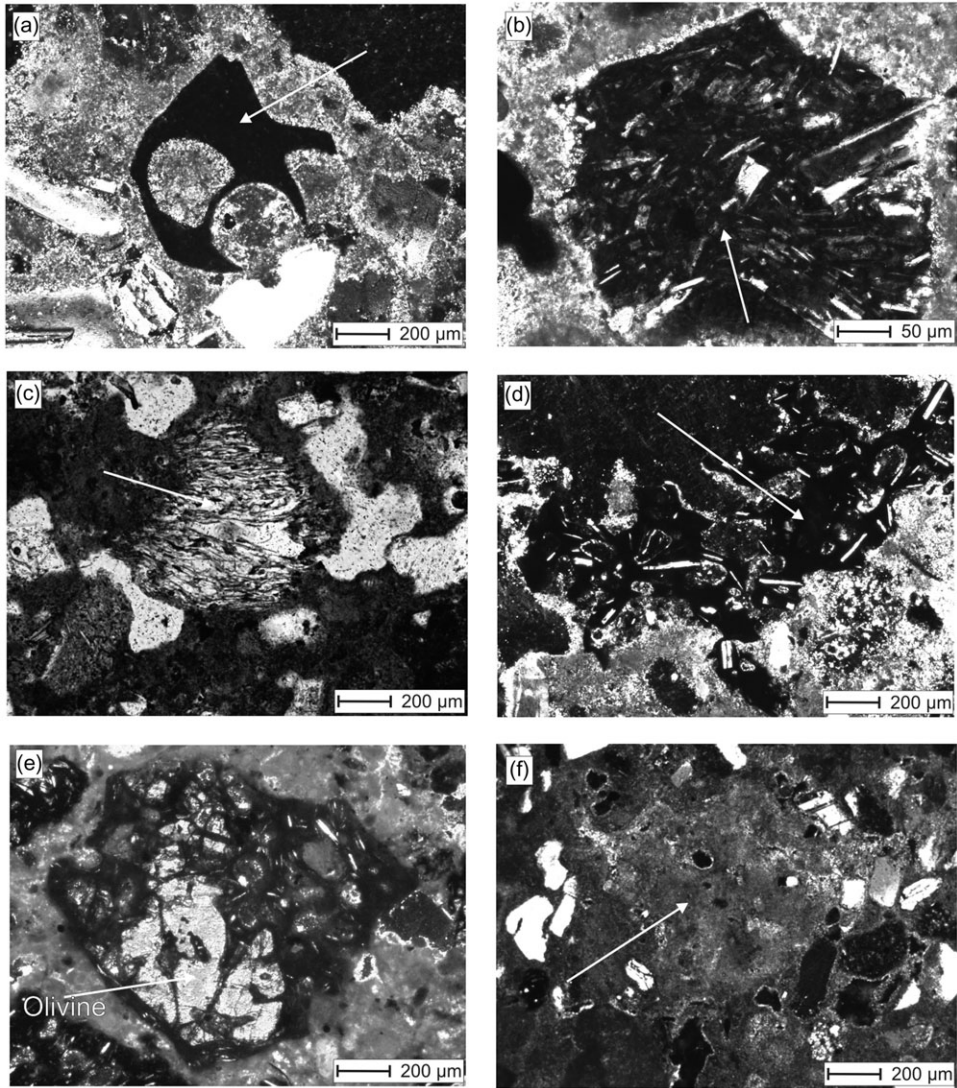
Figure 4 *(a) A shard in a microphotograph of sample TM1, under crossed polars. (b) Porphyric rhyolite in a microphotograph of sample TM1, under crossed polars. (c) Pumice in a microphotograph of sample TM2, under natural light. (d) Dark grey volcanic cinder in a microphotograph of sample TM6, under crossed polars. (e) Red volcanic cinder ('tezontle') in a microphotograph of sample TM20_II, under crossed polars. (f) A lump in a microphotograph of sample TM2, under crossed polars.*

Similarities and differences among the plasters coming from the construction phases

Taking into account the different construction phases, some slight differences can be observed. In the samples taken from phase II, only acid volcanic fragments (shards, pumices and porphyric rhyolites) were used in the aggregate. In the later construction phases, the volcanic materials are of both intermediate and acid origin (Fig. 6). Only samples TM11 (phase IV A), TM13 (phase IV
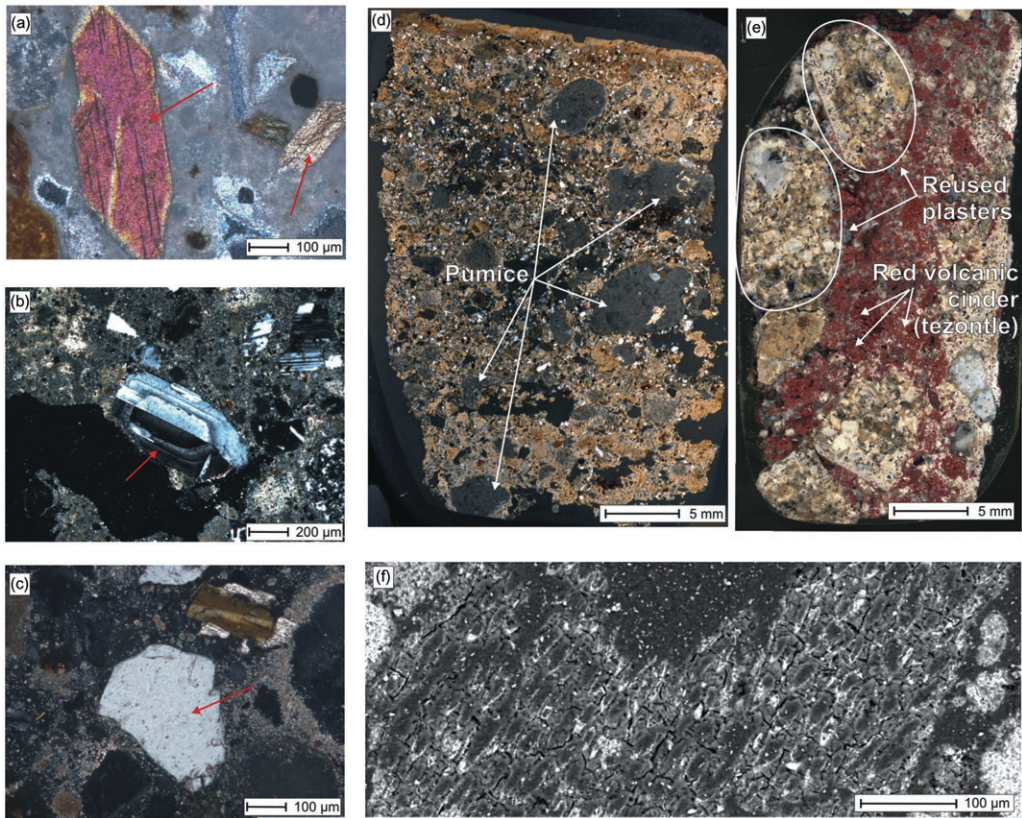
Figure 5 *(a) Amphibole in a microphotograph of sample TM1, under crossed polars. (b) Plagioclase in a microphotograph of sample TM9, under crossed polars. (c) Quartz in a microphotograph of sample TM15, under crossed polars. (d) A flatbed scanner image of sample TM6, under crossed polars. (e) A flatbed scanner image of sample TM14, under reflected light. (f) A SEM image of a charcoal fragment in sample TM3.*

B) and TM17_II (phase V) have exclusively acid materials. These data could be related to a different provenance of the raw materials used in the mixture. Samples from phase II and some samples from phase III (TM4 and TM5) show a good sorting of the particles, which suggests that the aggregate was probably sieved. This shows the good quality of the plasters. In the later construction phases, the sorting is generally poor (e.g., sample TM1 of phase II versus sample TM13 of phase IV B). Another difference between the samples is that red cinder only seems to be used from construction phase IV onward. The number of samples analysed for each construction phase is still limited, but it is already interesting that none of the samples of phases I, II and III contains this material. No red cinders are present in phase V.

In general, the differences between the phases are very subtle. The first impression it is that, apart from some elements ('*tezontle*' and sieving) there is a certain continuity in the techniques for making plasters. As for the samples coming from the same construction phases, the petrographic study has revealed some remarkable contrasts. The scheme presented in Figure 7 shows a summary of the different characteristics recorded, also showing the thin sections corresponding to the samples. Similar samples are enclosed inside an ellipse. Within phase II (TM1, TM2 and

Table 4	*SEM–EDS analysis of volcanic fragments*

|	SiO_2	TiO_2	Al_2O_3	FeO	MnO	MgO	CaO	Na_2O	K_2O	P_2O_5
TM1_R1	76.63	0.23	12.48	0.21	0.03	1.20	2.21	4.49	2.33	0.19
TM1_R2	76.36	0.24	13.02	0.92	0.12	0.72	0.48	4.18	3.90	0.06
TM2_R1	63.22	2.41	14.15	6.49	0.09	2.08	3.55	4.26	2.93	0.82
TM2_R2	73.61	0.29	15.09	1.63	0.11	1.16	1.81	3.80	2.32	0.18
TM3_R1	74.19	0.31	13.42	1.27	0.10	0.91	1.22	4.64	3.57	0.39
TM3_R2	76.23	0.40	5.54	2.18	0.18	1.21	2.82	3.98	7.42	0.05
TM3_R4	71.11	0.37	12.01	3.98	0.14	2.41	0.79	3.76	5.04	0.39
TM5_R3	72.86	0.25	14.66	0.96	0.04	1.04	2.59	4.86	2.35	0.39
TM6_R2	74.45	0.32	14.38	2.14	0.14	1.07	2.22	1.96	3.20	0.12
TM6_R3	61.82	1.66	15.05	5.52	0.20	3.55	4.41	5.48	1.39	0.94
TM6_R4	75.20	0.19	13.44	0.42	0.07	0.78	1.00	5.83	2.79	0.28
TM7_R1	55.84	1.54	17.81	6.25	0.20	3.91	7.61	4.86	1.05	0.94
TM7_R2	73.79	0.33	14.27	0.64	n.d.	0.81	2.37	3.80	3.63	0.36
TM7_R4	76.19	0.05	13.76	0.90	n.d.	0.73	1.75	3.22	3.31	0.08
TM8_R1	77.19	0.15	12.47	0.61	n.d.	0.95	1.27	2.97	4.21	0.18
TM8_R2	60.20	1.72	14.72	6.95	0.18	3.56	4.80	4.41	2.41	1.05
TM8_R4	75.15	0.16	13.63	0.29	n.d.	0.83	0.83	4.65	4.12	0.35
TM9_R1	74.69	0.24	13.97	0.35	0.04	0.76	1.68	4.78	3.24	0.26
TM9_R2	96.94	n.d.	0.96	n.d.	n.d.	0.67	0.07	0.85	0.15	0.36
TM9_R3	60.29	1.50	15.10	6.81	0.09	3.72	4.84	4.62	1.89	1.15
TM9_R4	75.73	0.13	12.56	1.01	0.06	0.72	0.50	4.93	4.16	0.20
TM10_R1	53.32	1.52	16.50	6.66	0.13	4.79	8.85	5.04	1.02	2.17
TM10_R2	72.38	0.27	14.67	1.45	0.16	0.77	1.57	5.10	3.35	0.27
TM10_R3	73.22	0.29	14.66	1.53	n.d.	1.13	2.24	4.01	2.50	0.41
TM11_R1	68.87	0.18	16.32	1.61	0.14	1.41	4.06	5.05	1.98	0.39
TM13_R1	72.79	0.11	14.31	1.72	n.d.	1.00	1.95	4.87	3.05	0.20
TM14_R1	55.49	1.94	15.63	7.49	0.21	5.30	6.51	4.97	1.52	0.94
TM14_R2	71.57	0.27	15.79	0.70	0.06	0.78	2.05	5.50	3.04	0.23
TM14_R3	74.18	0.19	14.42	1.40	n.d.	1.23	1.83	3.91	2.42	0.42
TM15_R1	64.80	0.13	20.58	0.58	0.09	0.76	4.11	6.97	1.75	0.23
TM15_R2	53.72	2.13	16.72	8.58	0.27	5.00	6.53	5.61	0.59	0.85
TM15_R3	75.36	0.40	12.33	1.46	0.07	1.04	4.21	0.91	3.92	0.29
TM16_R1	61.50	2.26	14.19	6.95	0.23	3.04	4.55	4.03	2.40	0.84
TM16_R2	59.15	2.18	14.02	8.64	0.19	4.39	4.72	3.42	2.45	0.84
TM17_I_R1	58.61	1.13	18.75	4.89	0.08	2.34	6.06	5.38	1.95	0.81
TM17_II_R1	72.33	0.29	14.63	0.99	0.07	0.92	2.17	5.20	2.92	0.46
TM19_R1	58.33	1.25	16.58	5.57	0.13	3.39	6.25	5.49	1.94	1.08
TM19_R2	54.40	1.21	18.77	5.66	0.14	2.86	9.50	5.28	1.28	0.90
TM20_I_R1	60.50	1.46	15.31	6.50	0.20	4.30	3.51	5.23	1.87	1.10
TM20_I_R2	57.60	0.24	25.19	1.23	0.08	1.05	6.95	6.64	0.56	0.46
TM20_I_R3	59.22	1.79	14.26	7.30	0.19	4.42	5.04	4.59	2.23	0.96
TM20_I_R4	75.51	0.25	12.61	0.98	0.15	0.81	0.51	4.54	4.37	0.28
TM20_II_R1	58.14	1.09	19.82	4.26	0.17	2.17	6.11	5.34	2.05	0.85
TM20_II_R2	56.24	0.65	23.27	3.57	0.17	2.00	7.63	5.32	0.85	0.31
TM20_II_R3	57.98	0.20	25.10	1.17	0.07	0.91	7.60	5.91	0.80	0.28
TM20_II_R4	75.33	0.15	12.42	1.05	0.10	0.82	0.52	4.41	4.85	0.35

n.d., Not determined.
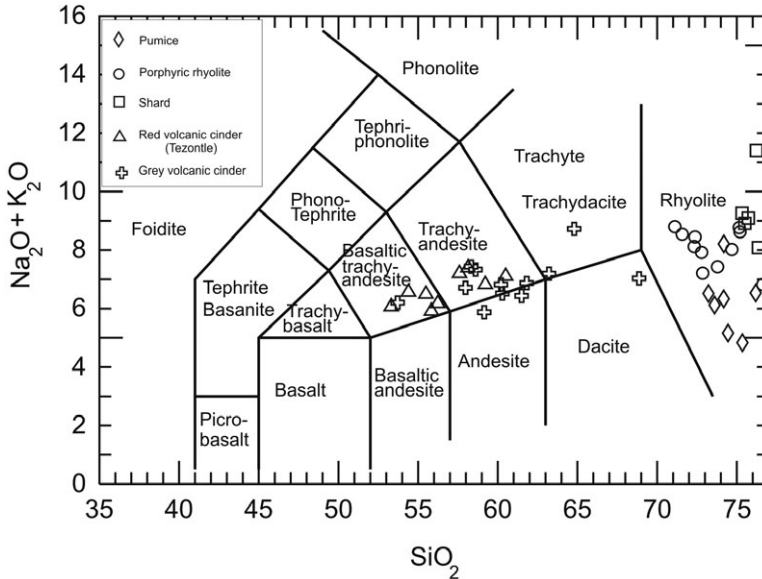
Figure 6 *Classification of the volcanic rocks inside the plasters by means of a TAS diagram (Le Maitre* et al. *2005).*

TM3), it is possible to detect a small, but significant, difference between sample TM3 and the two remaining samples. In sample TM3, the mean size of the aggregate is smaller than that of samples TM1 and TM2 (Fig. 7 (a)). In phase III (TM4, TM5 and TM6), sample TM6 contrasts with the others due to the characteristic presence of pumices, whose dimensions are generally more than 5 mm (Figs 5 (d) and 7 (b)). In phase IV (TM7, TM8 and TM9), sample TM7 is the only one to have red cinders (Fig. 7 (c)). Also in phase IV A, the main difference between samples TM10 and TM11 lies in the presence of red cinders in sample TM10 (Fig. 7 (d)). In phase IV B, sample TM14 is the only one to contain red cinders and reused plaster fragments (Figs 5 (e) and 7 (e)), while sample TM13 has no red cinders. In phase V (Fig. 7 (f)), sample TM15 is the only one with pumice fragments, and the aggregate of sample TM16 has mean dimensions larger than those of sample TM17. In phase VI, sample TM19 is the only one containing grey cinders, although it is the sample that contains them in minor quantities (Fig. 7 (g)). Sample TM20, which belongs to phase VII, is composed only of two layers of '*firme*'. Both layers have red cinders, but in the interior layer (sample TM20_II) the cinders have mean sizes larger than those of the exterior layer (sample TM20_I) (Fig. 7 (h)). As said above, in sample TM14 it is possible to observe the reuse of plaster belonging to previous construction phases. This is not a common phenomenon, but it was also observed in one sample coming from Teotihuacan, where an earthen material was incorporated in the plaster of a sample from the floor of the central patio of the '*centro de barrio*' Teopancazco (Barba *et al.* 2009). The reused plasters of sample TM14 are very similar to the plasters of samples TM8 and TM9 from the previous construction phase IV.

In general, there are differences within the same construction phases. They are mainly based on the presence/absence of cinders, and other raw materials in the aggregate. Although some of the differences could be attributed to different mixtures used for the various construction elements (staircases, floors, balustrades and walls), we do not have elements to support this hypothesis. As a matter of fact, in some cases samples that are compositionally similar belong to
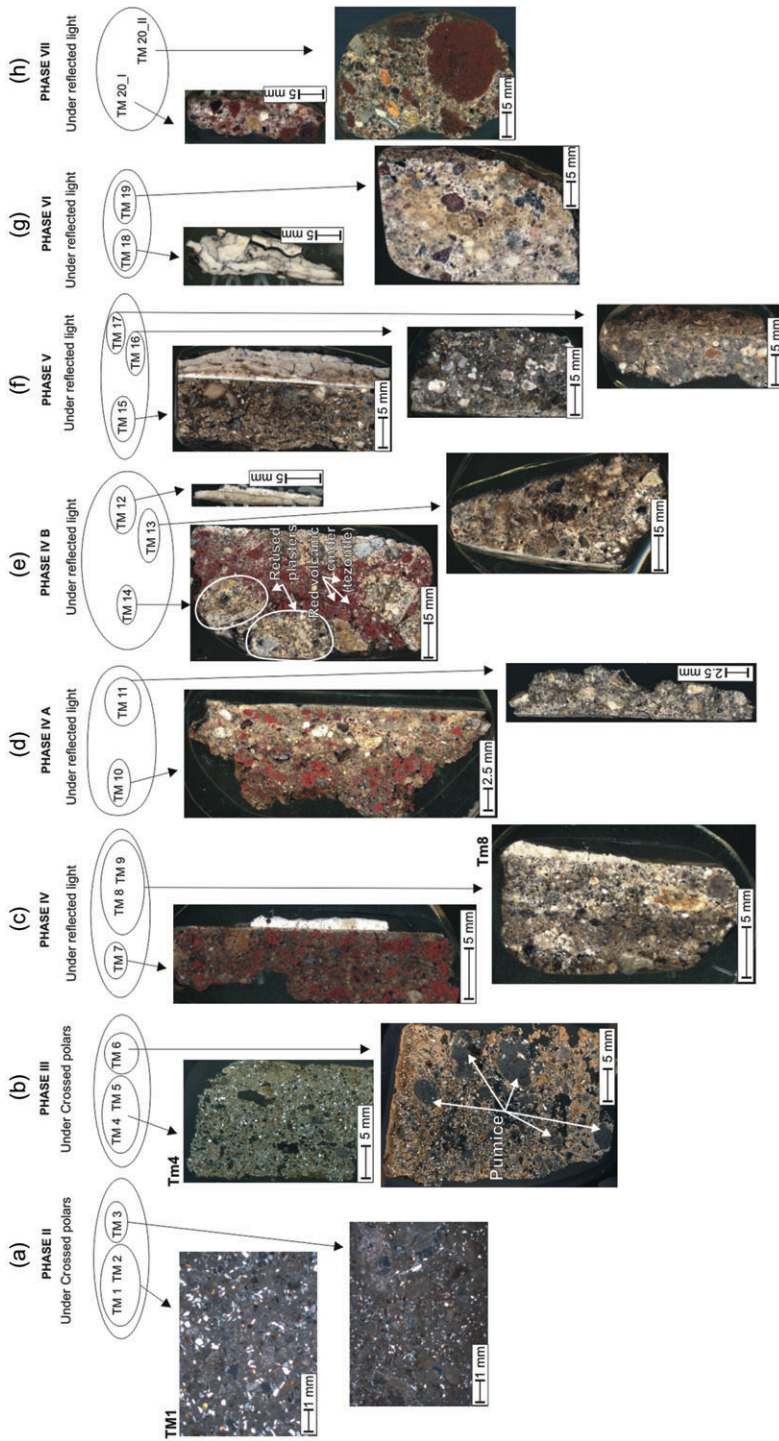
Figure 7   *Analogies between and differences among the plasters in the various construction phases.*

different architectural structures, such as samples TM1 and TM2, which are petrographically similar, but were sampled from a floor and a wall, respectively (Table 2). In the same direction, samples coming from the same architectural features show differences in time and space (e.g., samples TM1 [phase II], TM6 [phase III], TM10 [phase IV A] and TM14 [phase IV B], which come from floors). The differences could therefore be due to a difference in the raw materials used and/or to the participation of different workers in the building process. A study of the possible outcrops of all the raw materials used as aggregate in the plasters should be performed in order to better understand this problem.

Provenance of the limestone used in the plasters in Templo Mayor by LA–ICP–MS and SEM–EDS analyses

To establish the provenance of the limestone used to make the plasters of the Templo Mayor samples, the methodology proposed in Barba *et al*. (2009) was applied. This methodology is based on the compositional similarities between the lumps (Bakolas *et al*. 1995) and the limestone used to produce the lime for plasters. In particular, a preliminary SEM–EDS study allowed us to recognize a variable number of lumps (from 1 to 5) for each sample—except for sample TM4, in which they were absent. In a subsequent step of our study, a variable number of LA–ICP–MS analyses were carried out on each lump in relation to their dimension. Tables 5 and 6 list, for each lump, the mean value of analytical data for major and trace elements determined, respectively, by the SEM–EDX and LA–ICP–MS methods.

The 46 lumps analysed in the 19 studied samples show a moderate compositional heterogeneity, with concentrations of CaO ranging from 77% to 94.6% and concentrations of SiO_2 ranging from 3% to 14%. Only the lumps TM2-4, TM1-1 and TM11-1 are very different, showing low concentrations of CaO and high concentrations of SiO_2 (Table 5). Also, the trace (Sc, V, Cr, Co, Ni, Zn, Rb, Sr, Y, Zr, Nb, Ba, Pb and U) and rare earth (La, Ce and Pr) elements show a limited variability. In particular, all the analysed lumps show La/Ce always less than 1 and U/Pb less than 1, with the exception of a small group of lumps that show U/Pb ranging from 1 to 4 (Table 6). Nevertheless, since the geochemical variability can be observed between lumps of the same samples, it is reasonable to attribute the heterogeneity of the lumps to the heterogeneity of the source.

The results of the analyses of the lumps were compared with the analyses of the samples collected on the six limestone outcrops present in the surroundings of the Basin of Mexico (Barba and Córdova 1999, 2010). The outcrops are located in the modern state of Hidalgo, near Tula (Cav9, Fig. 8), in the state of Puebla (Cav8) and in the state of Morelos (Cav1, Cav2, Cav3 and Cav4). The limestone that comes from these outcrops has already been characterized in previous work done by our group that was aimed at identifying the provenance of the limestone used in the fabrication of the plasters of the floors of the Teopancazco quarter temple at Teotihuacan (Barba *et al*. 2009). The two cities (Teotihuacan and Tenochtitlan) were in fact both located in the Basin of Mexico and potentially had access to the same outcrops.

The results obtained with the analysis of the lumps (Fig. 8 (a)) were plotted on the diagrams, which better discriminate the geological samples of the different outcrops (Barba *et al*. 2009). In particular, in the diagram of SiO_2 versus CaO (Fig. 8 (b)), all of the lumps plot in the same area of the limestone samples coming from the Tula outcrop. Similarly, the diagrams for Ni versus La/Ce (Fig. 8 (c)) and U/Pb versus La/Ce (Fig. 8 (d)) confirm that the composition of the lumps of all studied samples from the Tenochtitlan's Templo Mayor overlap with the composition of Tula's limestone. Indeed, all of the lumps studied in the 19 samples show the same geochemical

Table 5   *SEM–EDS analysis of lumps in the plasters*

Sample	TM1			TM2			TM3		TM5				TM6			TM7		TM8
Lumps, N	1	2	3	1	3	4	1	2	1	2	3	4	1	2	3	1	3	2
SiO_2	17.95	10.69	2.61	20.78	8.22	8.39	3.75	5.65	14.10	12.59	3.77	5.77	11.56	10.96	8.92	5.31	3.76	6.53
Al_2O_3	2.71	1.77	0.78	2.03	1.28	1.16	1.01	1.21	1.80	0.73	0.46	0.87	2.28	3.36	2.10	1.09	0.96	1.43
Fe_2O_3	n.d.	n.d.	n.d.	n.d.	n.d.	n.d.	n.d.	n.d.	n.d.	n.d.	n.d.	n.d.	1.81	1.42	0.98	n.d.	n.d.	n.d.
MgO	6.53	3.52	3.31	6.84	3.70	2.96	5.66	2.77	6.39	5.44	2.52	3.05	3.69	2.54	2.92	2.10	1.91	2.59
CaO	69.67	82.01	90.63	67.57	83.80	83.21	87.59	88.19	77.04	80.00	91.95	89.22	80.66	81.71	85.08	88.14	90.93	85.13
Na_2O	1.26	0.58	0.48	1.33	1.10	1.16	0.93	0.78	n.d.	0.27	0.60	n.d.	n.d.	n.d.	n.d.	0.74	0.61	0.88
K_2O	n.d.	n.d.	n.d.	n.d.	n.d.	n.d.	n.d.	n.d.	n.d.	n.d.	n.d.	n.d.	n.d.	n.d.	n.d.	n.d.	n.d.	n.d.
P_2O_5	1.88	1.43	2.19	1.44	1.90	1.81	1.06	1.41	0.67	0.97	1.00	1.09	n.d.	n.d.	n.d.	1.40	1.12	2.01
SO_3	n.d.	n.d.	n.d.	n.d.	n.d.	2.40	n.d.	n.d.	n.d.	n.d.	n.d.	n.d.	n.d.	n.d.	1.22	1.43	1.32	0.90

Sample	TM9			TM10		TM11			TM12	TM13			TM14		
Lumps, N	1	2	3	1	2	1	2	3	3	1	2	3	1	2	3
SiO_2	6.48	11.60	14.15	8.88	7.65	15.09	8.21	8.71	8.43	5.94	4.33	5.36	12.65	8.71	4.90
Al_2O_3	1.36	1.04	0.19	0.79	1.83	2.73	2.30	2.76	n.d.	n.d.	n.d.	n.d.	3.24	2.42	1.71
Fe_2O_3	n.d.	n.d.	n.d.	n.d.	n.d.	1.05	0.57	0.55	n.d.	n.d.	n.d.	n.d.	n.d.	n.d.	n.d.
MgO	2.67	4.98	1.66	1.58	2.05	4.82	3.14	1.64	1.47	1.59	0.91	1.02	1.53	1.36	2.99
CaO	85.93	77.51	80.40	85.66	83.16	71.93	81.52	82.58	89.58	92.47	94.65	93.28	82.58	87.51	90.41
Na_2O	0.57	0.64	1.53	0.33	1.01	2.33	1.60	1.42	0.52	n.d.	0.12	0.35	n.d.	n.d.	n.d.
K_2O	n.d.	n.d.	n.d.	n.d.	n.d.	0.67	0.61	0.61	n.d.	n.d.	n.d.	n.d.	n.d.	n.d.	n.d.
P_2O_5	1.67	1.22	0.94	1.09	1.90	1.38	2.05	1.72	n.d.	n.d.	n.d.	n.d.	n.d.	n.d.	n.d.
SO_3	3.00	1.31	1.68	n.d.	n.d.	n.d.	n.d.	n.d.	n.d.	n.d.	n.d.	n.d.	n.d.	n.d.	n.d.

Sample	TM15			TM16			TM17			TM18	TM19	TM20	
Lumps, N	1	3	5	1	2	4	2	3	4	1	1	1	2
SiO_2	5.34	5.82	9.30	9.17	10.24	8.07	6.49	11.55	4.68	3.88	5.52	5.18	4.24
Al_2O_3	1.85	1.55	1.77	2.73	2.96	2.85	2.52	3.84	1.84	1.03	1.20	1.57	1.33
Fe_2O_3	n.d.	n.d.	n.d.	n.d.	n.d.	n.d.	n.d.	n.d.	n.d.	n.d.	n.d.	n.d.	n.d.
MgO	1.10	1.20	1.09	1.53	3.93	2.48	1.74	2.17	1.34	2.76	1.26	1.34	0.91
CaO	91.71	91.42	87.83	85.59	81.62	85.50	89.26	82.44	92.13	92.33	92.03	90.89	92.57
Na_2O	n.d.	n.d.	n.d.	0.43	0.58	0.76	n.d.	n.d.	n.d.	n.d.	n.d.	0.68	0.65
K_2O	n.d.	n.d.	n.d.	n.d.	n.d.	n.d.	n.d.	n.d.	n.d.	n.d.	n.d.	n.d.	n.d.
P_2O_5	n.d.	n.d.	n.d.	n.d.	n.d.	n.d.	n.d.	n.d.	n.d.	n.d.	n.d.	n.d.	n.d.
SO_3	n.d.	0.55	0.68	0.34	n.d.	n.d.	n.d.	n.d.	n.d.	n.d.	n.d.	n.d.	n.d.

n.d., Not determined.

Table 6   *ICP–MS laser ablation analysis of lumps in the plasters*

Sample	TM1		TM2			TM3		TM5				TM6			TM7		TM8
Lumps, N	1	2	1	2	3	1	2	1	2	3	4	1	2	3	1	3	2
Sc	3.46	2.52	2.83	0.50	1.51	2.97	1.11	1.61	0.87	0.98	n.d.	4.11	1.52	0.95	0.74	1.51	n.d.
V	57.98	23.46	4.03	7.93	24.35	8.49	14.91	9.55	32.59	8.73	12.80	21.69	11.38	12.19	6.21	13.03	13.22
Cr	11.57	32.62	25.77	9.07	18.90	8.47	n.d.	n.d.	n.d.	13.77	n.d.	22.28	3.50	n.d.	5.84	8.78	3.23
Co	4.49	1.85	2.21	3.48	5.89	1.09	4.15	1.68	15.53	1.24	2.51	14.01	1.51	3.52	0.89	1.58	1.59
Ni	17.56	4.98	4.68	5.58	12.92	2.25	4.13	3.63	11.80	2.02	4.37	6.75	3.05	2.79	3.29	4.98	2.29
Zn	134.78	17.46	43.25	17.97	21.37	4.72	10.86	3.50	24.00	4.85	8.93	24.99	6.80	6.51	10.46	7.16	4.76
Rb	31.38	5.84	3.51	2.97	9.73	1.10	1.47	1.35	6.18	0.52	2.01	20.47	7.94	3.61	0.61	1.53	1.34
Sr	3479	2818	2658	1753	1930	3597	1719	1053	2504	662	1199	2019	1961	1002	1070	946	1210
Y	3.20	1.54	0.78	1.53	2.34	0.95	3.63	0.57	5.88	0.41	0.80	4.46	2.44	0.50	0.55	0.90	0.50
Zr	44.25	10.69	5.62	5.70	19.58	3.60	4.91	5.85	7.83	3.08	7.60	49.50	12.84	3.80	4.38	4.13	3.45
Nb	2.47	0.48	0.56	0.23	0.88	0.20	0.15	0.35	0.24	0.09	0.39	1.88	0.37	0.24	0.12	0.32	0.17
Ba	1106	386	457	359	472	908	313	210	737	165	262	721	493	289	92	138	196
La	3.98	1.54	0.92	1.19	2.69	0.42	1.91	0.53	7.08	0.27	0.75	8.18	2.52	0.31	0.30	0.84	0.42
Ce	7.53	3.15	1.76	2.44	5.99	0.72	6.58	0.96	12.82	0.72	1.34	15.01	6.05	0.66	0.43	1.69	0.75
Pr	1.04	0.46	0.49	0.31	0.70	0.11	0.42	0.11	1.91	0.04	0.16	1.65	0.71	0.05	0.10	0.17	0.08
Pb	5.67	0.91	1.25	0.76	2.22	0.46	1.56	0.64	0.68	0.66	0.49	5.18	1.22	0.69	31.95	12.84	0.25
U	2.38	0.59	1.18	0.54	0.54	0.67	1.45	0.65	3.29	0.73	0.83	1.30	0.79	0.61	1.84	1.54	1.25

Sample	TM9			TM10		TM11			TM12	TM13			TM14		
Lumps, N	1	2	3	1	2	1	2	3	3	1	2	3	1	2	3
Sc	1.41	1.65	1.36	1.54	1.98	1.06	0.73	9.67	n.d.	n.d.	3.87	1.64	1.42	0.92	3.73
V	24.65	16.29	7.33	18.52	23.48	31.93	13.72	62.70	23.55	13.22	30.14	11.55	12.43	10.86	4.42
Cr	4.73	3.25	5.58	8.97	8.45	10.43	3.69	20.10	17.07	5.38	23.41	6.92	n.d	7.55	19.77
Co	1.63	54.48	0.59	4.62	7.57	5.97	1.75	35.60	0.90	11.38	1.92	5.88	1.28	8.07	7.51
Ni	3.37	3.52	2.60	8.54	5.95	7.58	3.76	11.62	2.29	3.39	6.48	2.77	3.82	4.55	3.20
Zn	11.85	15.21	9.62	13.02	11.66	21.76	4.96	6.22	23.08	5.41	22.96	6.14	14.93	16.93	11.32
Rb	2.76	3.38	1.28	5.39	8.32	9.73	3.41	24.35	1.52	2.56	20.82	2.89	12.88	5.03	3.22
Sr	1219	815	1259	2396	2218	1570	1352	1588	848	773	497	1303	1142	1124	2488
Y	1.89	1.30	5.74	9.53	2.58	1.55	0.74	6.33	3.34	1.86	5.00	7.18	2.23	1.12	1.37
Zr	16.69	13.69	5.72	10.19	15.44	12.84	3.68	20.57	8.19	4.88	18.94	13.78	10.88	4.61	7.85
Nb	0.54	0.44	0.22	0.40	0.60	0.64	0.10	1.12	0.30	0.21	1.53	0.64	0.36	0.25	2.16
Ba	328	309	244	419	584	597	377	744	183	298	290	635	362	357	690

Table 6   (*Continued*)

Sample	TM9				TM10		TM11			TM12		TM13		TM14		
Lumps, N	1	2	3	4	1	2	1	2	3	1	3	2	3	1	2	3
La	1.55	1.53	0.81	0.27	4.88	2.25	5.61	0.64	11.47	0.86	2.04	3.77	6.92	2.52	1.09	1.33
Ce	4.03	3.68	1.46	0.49	12.09	6.13	10.58	1.07	14.93	2.81	3.15	8.36	11.88	4.72	2.64	2.18
Pr	0.46	0.39	0.14	0.04	1.48	0.66	1.14	0.12	2.82	0.18	0.46	1.43	1.59	0.60	0.15	0.28
Pb	0.58	0.56	7.20	8.05	0.90	1.16	2.52	1.26	7.99	0.57	12.64	5.14	0.75	2.24	2.99	0.80
U	1.52	1.17	2.27	1.56	1.67	1.10	1.30	1.34	1.49	1.30	1.71	1.15	3.05	0.99	4.04	0.29

| Sample	TM15			TM16			TM17			TM18	TM19	TM20	
Lumps, N	1	3	5	1	2	4	2	3	4	1	1	1	2
Sc	1.41	1.37	2.34	2.99	1.89	1.25	n.d.	2.06		0.90	1.07	0.66	1.89
V	12.05	9.79	23.48	8.54	21.61	14.05	7.86	10.51	13.35	42.02	23.63	10.46	10.83
Cr	8.45	5.62	5.91	6.29	26.57	4.25	n.d.	14.17	5.03	15.62	4.57	3.32	7.70
Co	0.66	1.14	19.30	1.63	1.19	0.53	0.70	0.83	0.77	1.70	3.97	1.65	1.25
Ni	1.20	1.69	4.46	3.50	6.45	8.72	6.87	14.18	7.80	3.62	7.07	2.86	4.43
Zn	10.51	9.97	12.73	6.38	10.86	5.07	6.08	6.16	107.52	4.60	5.87	46.56	7.56
Rb	6.12	12.35	40.10	7.01	3.01	2.61	0.81	3.58	1.60	4.10	0.21	6.79	10.60
Sr	385	212	682	366	275	195	78	364	103	1628	1313	351	1142
Y	2.35	1.41	6.16	2.64	2.29	0.90	0.60	1.12	1.50	0.52	2.25	1.46	1.82
Zr	3.57	8.09	28.84	6.86	7.60	10.93	2.11	3.75	2.60	2.73	4.61	2.18	6.03
Nb	0.16	0.45	2.29	0.25	0.45	0.31	0.13	0.33	0.13	0.22	0.24	0.13	0.37
Ba	123	114	342	292	143	169	25	133	183	168	184	82	87
La	1.64	1.57	6.32	1.72	1.98	1.01	0.50	0.90	0.69	0.48	1.94	1.45	1.74
Ce	3.24	3.04	9.88	3.47	3.08	1.98	0.97	1.95	1.30	0.66	3.21	2.85	3.08
Pr	0.33	0.34	1.30	0.54	0.54	0.16	0.15	0.23	0.18	0.11	0.35	0.33	0.40
Pb	0.67	0.85	2.17	1.41	1.25	0.82	0.57	2.14	1.25	0.61	1.17	10.27	1.41
U	0.44	0.30	0.71	0.80	0.90	0.65	0.36	1.45	0.53	0.64	0.87	0.43	0.59

n.d., Not determined.
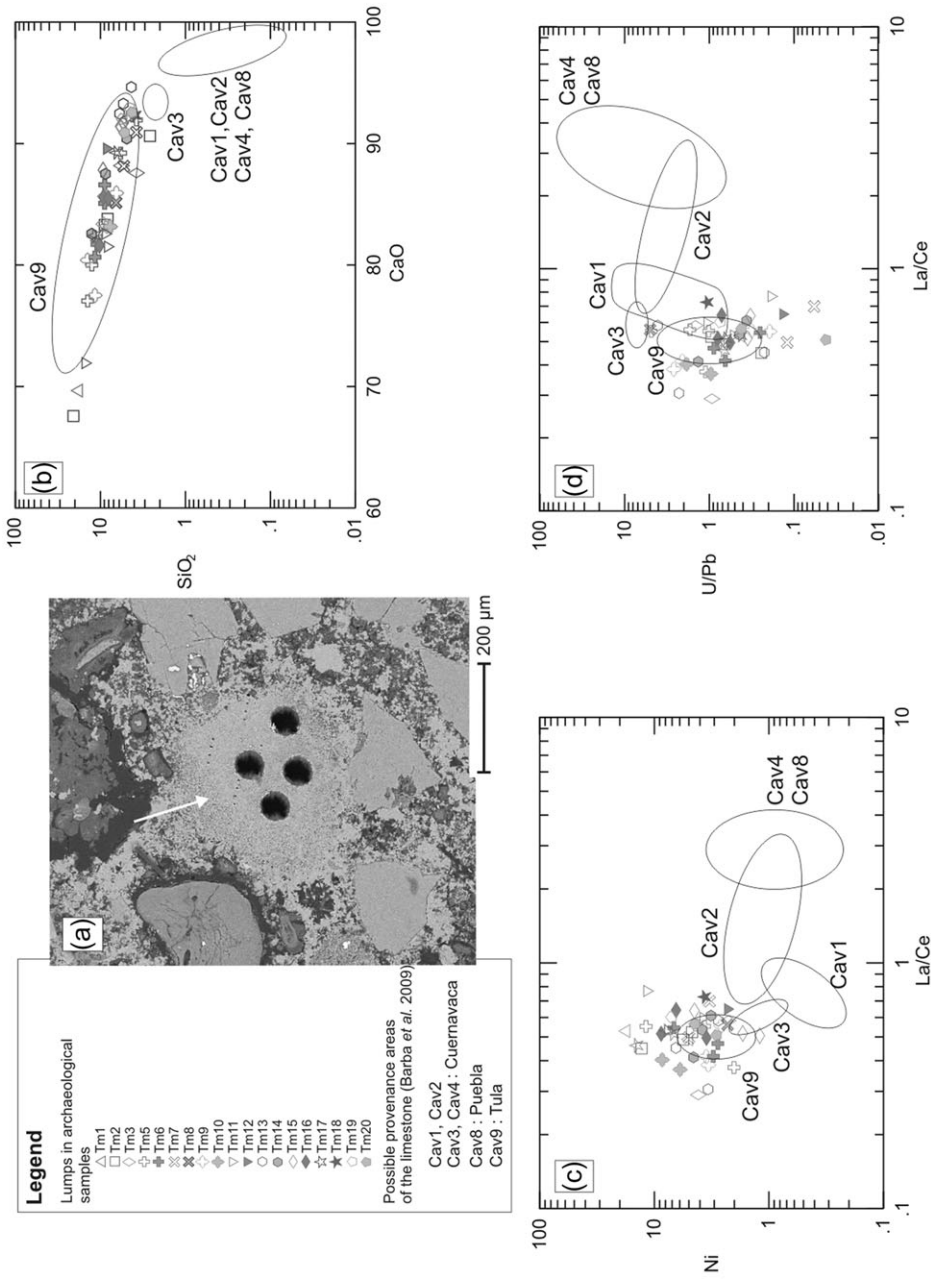
Figure 8 (a) A SEM image of a lump in sample TM5: circular holes produced by ICS–MS laser ablation can be seen inside the lump. (b) SiO_2 versus CaO. (c) Ni versus La/Ce. (d) U/Pb versus La/Ce. The ellipses enclose the compositional group of possible mining areas of the limestone (Barba et al. 2009): the compositional data for the Tula limestone and the Templo Mayor lumps overlap.

characteristic, confirming that no differences exist among the construction phases in the limestone used. This means that the limestone used in the parts of the Templo Mayor that were sampled and analysed came from the Tula region.

CONCLUSIONS

No differences can be observed in the limestone provenance between the different construction phases and within the same construction phase. The geochemical results for both the major elements and the trace elements show that Tula is the source area of the limestone used in the Templo Mayor plasters. The provenance of the limestone used to cover the pyramid of the Templo Mayor is the same as that of the limestone used in the construction of the central patio of Teopancazco, in Teotihuacan (Barba *et al*. 2009), although the two buildings were built by different people and with a time difference of several centuries. While, in the Teotihuacan, the choice of Tula limestone was possibly due to the proximity of the outcrops, in the case of Tenochtitlan, all the three outcrops were more or less at the same distance. However, we have to remember that travelling to Puebla and Cuernavaca required the considerable effort of crossing very high mountain ranges, while the route to Tula traversed a relatively flat area. Nevertheless, it is also possible that the people from Teotihuacan and/or Tenochtitlan had realized that the limestone coming from the Tula region provided the possibility of obtaining a plaster with better hydraulic properties (Taylor 1997; Ubbríaco and Tasselli 1998) than the other outcrops, due the fact that the limestone coming from Tula is richer in SiO_2, Al_2O_3 and Fe_2O_3 (Barba *et al*. 2009). These elements react to form calcium silicate hydrates, commonly called C–S–H phases, which make the plasters more resistant to degradation.

Although the provenance of the limestone used in the Templo Mayor (Tenochtitlan) and in the Teopancazco (Teotihuacan) temple is the same, the samples from the two archaeological sites are completely different. In fact, in the Teotihuacan samples, the lime is present only in the '*enlucido*', while in Templo Mayor it is also present in the lower layer ('*firme*'). Furthermore, in the Teotihuacan samples volcanic glass shards are the main aggregate, with traces of other minerals (Barba *et al*. 2009), while in the Templo Mayor samples there are mainly volcanic cinders, pumices, plagioclase, amphibole, olivine, and traces of quartz and shard. Therefore the origin of the aggregate materials used in the two archaeological sites is completely different.

The fact that Tula is the source area of the limestone used in the Templo Mayor plasters is an interesting issue. As stated in the introduction, after the historical sources written during the 16th century, the Aztecs imported, by way of tribute and commerce, lime and limestone from different regions. As said above, Friar Diego Durán (1984: see also Nicholson 1987; López Luján *et al*. 2003; López Luján 2006) reports that for the enlargement of the Templo Mayor ordered by King Motecuhzoma I around AD 1467, the neighbouring cities would bring stone and would contribute to the building of one of the façades: Texcoco that of the west, Chalco that of the south, Tlacopan that of the east and Xochimilco that of the north. The people from the Toluca Valley would bring supplies of sand, while those from the Cuernavaca area (in the modern state of Morelos) would provide the lime. However, differences in the building materials or techniques are not perceptible in the façades that form part of each of the Templo Mayor's phases. Moreover, our analyses show that no lime from Morelos was used in the northern façade corresponding to this construction phase, as happens with the rest of the samples, all of them being from the Tula region. This could be explained either by thinking that Durán was not well informed about this historical event, or by suggesting that possibly the lime that they provided was not used for the building of the northern façade of that phase.

It is worth saying that no traces of limestone coming from other outcrops mentioned in the historical sources are present in our samples. For instance, no limestone comes from the state of Puebla, although the tributary lists known as the *Matrícula de Tributos* (1991, 22) and the *Codex Mendoza* (1992, 28r, 42r) record that lime loads were brought periodically from Tepeacac (a province located in the modern state of Puebla), showing a possible different use for that limestone. Instead, it is interesting that Sahagún (2000, 1132), mentions that the limestone used to paint, and called '*tetizatl*' (lime of stone), was obtained 'in the small rivers near Tula'. Although he does not mention the use of this limestone for the production of plasters, it is possible that it was used for this purpose, while the limestone coming from Morelos and other areas could possibly have had different uses, such as the '*chimaltizatl*' that was used in paint and that came from Huaxtepec (near Cuernavaca, Morelos) and was sold in the market. On the other hand, Gibson (1991, 343) states that in the 16th century, at the beginning of the Colonial period, it was difficult to get limestone in Mexico City. The author quotes that lime was produced in 'Zumpango, Citlaltépec, Xaltocan, Hueypoxtla y Tequixquiac', and in particular 'the burning of the limestone in Hueypoxtla became an important industry'. At the end of the Colonial period, most of the lime for the capital of New Spain was obtained from the region of Tula. Therefore, this quote also shows that Tula was an important place of origin of the limestone. Here, limestone outcrops are present in different places near the modern villages of Santa María Apaxco, Apaxco de Ocampo, Hueypoxtla, Santiago Tequixquiac and Tlapanaloya—and continuity in the use of the outcrops is evident from the fact that the modern villages overlap with those of the 16th century.

Concerning the study of the building techniques at Templo Mayor, the use of the red cinders from phase IV onward could be explained as evidence for the understanding that the plaster mixture obtained by adding the cinders has a better quality due to the pozzolanic properties of this volcanic material (Moropoulou *et al.* 2004). The introduction of this material, which comes from small volcanic cones in the Basin of Mexico, and therefore of an innovative way of preparing plaster, happens at the same time as an important political change occurs in the Aztec world. In fact, this is the moment at which the Aztecs gained independence and control over their people and resources. This new situation is reflected in the works of art—both in the quantity of the raw materials that arrived in Tenochtitlan and in the better quality of the artefacts (López Luján 2006; López Austin and López Luján 2009).

The study of plaster samples coming from other buildings of the Sacred Precinct of Tenochtitlan is under way, in order to verify the provenance of the limestone used in the making of the lime, and their construction characteristics. Future studies will be directed to understanding the provenance of '*tezontle*' and the other raw materials present in the aggregates of the plasters.

REFERENCES

Bakolas, A., Biscontin, G., Moropoulou, A., and Zendri, E., 1995, Characterization of the lumps in the mortars of historic masonry, *Thermochimica Acta*, **269/270**, 809–16.

Barba, L., and Córdova, J. L., 1999, Estudios energéticos de la producción de cal en tiempos Teotihuacanos y sus implicaciones, *Latin American Antiquity*, **10**, 168–79.

Barba, L., and Córdova, J. L., 2010, *Materiales y energía en la arquitectura de Teotihuacan*, IIA, UNAM, México.

Barba, L., Blancas, J., Manzanilla, L. R., Ortiz, A., Barca, D., Crisci, G. M., Miriello, D., and Pecci, A., 2009, Provenance of the limestone used in Teotihuacan (Mexico): a methodological approach, *Archaeometry*, **51**, 525–45.

Barca, D., De Francesco, A. M., and Crisci, G. M., 2007, Application of laser ablation ICP–MS for characterization of obsidian fragments from peri-Tyrrhenian area, *Journal of Cultural Heritage*, **8**, 141–50.

Carò, F., Riccardi, M. P., and Mazzilli Savini, M. T., 2008, Characterization of plasters and mortars as a tool in archaeological studies: the case of Lardirago Castle in Pavia, northern Italy, *Archaeometry*, **50**, 85–100.

Codex Mendoza, 1992, University of California Press, Berkeley, CA.

Crisci, G. M., Franzini, M., Lezzerini, M., Mannoni, T., and Riccardi, M. P., 2004, Ancient mortars and their binder, *Periodico di Mineralogia*, **73**, 259–68.

Crisci, G. M., Davoli, M., De Francesco, A. M., Gagliardi, F., Mercurio, P., and Miriello, D., 2001, L'analisi composizionale delle malte: metodo di studio delle fasi costruttive in architettura, *Arkos*, **4**, 36–41.

Crisci, G. M., Davoli, M., De Francesco, A. M., Gagliardi, F., Gattuso, C., Mercurio, P., and Miriello, D., 2002, L'analisi composizionale delle malte, un valido mezzo per risalire alle fasi costruttive. Risultati preliminari, in *Proceedings of II Congresso Nazionale di Archeometria*, 485–94.

Damiani, D., Gliozzo, E., Memmi Turbanti, I. and Spangenberg, J. E., 2003, Pigments and plasters discovered in the house of Diana (Cosa, Grosseto, Italy): an integrated study between art history, archaeology and scientific analyses, *Archaeometry*, **45**, 341–54.

Durán, D., 1984, *Historia de las Indias de Nueva España e islas de la tierra firme*, vol. 2, 225–8, Porrúa, Mexico.

Fallon, S. J., White, J. C., and McCulloch, M. T., 2002, Porites corals as recorders of mining and environmental impacts: Misima Island, Papua New Guinea, *Geochimica et Cosmochimica Acta*, **66**, 45–62.

Franzini, M., Leoni, L., Lezzerini, M., and Sartori, F., 2000, The mortar of the 'Leaning Tower' of Pisa: the product of a medieval technique for preparing high strength mortars, *European Journal of Mineralogy*, **12**, 1151–63.

Fryer, B. J., Jackson, S. E., and Longerich, H. P., 1995, The design, operation and role of the laser-ablation microprobe coupled with an inductively coupled plasma-mass spectrometer (LAM–ICP–MS) in the Earth sciences, *The Canadian Mineralogist*, **33**, 303–12.

Gibson, C., 1991, *Los aztecas bajo el dominio español 1519–1810*, Siglo XXI, 11th edn, Mexico.

Graulich, M., 1987, Les incertitudes du Grand Temple, in *Les aztèques. Trésors du Mexique Ancien*, vol. 2, 121–31, Roemer und Pelizaeus Museum, Wiesbaden.

Gunther, D., and Heinrich, C. A., 1999, Enhanced sensitivity in laser ablation-ICP mass spectrometry using helium–argon mixtures as aerosol carrier, *Journal of Analytical Atomic Spectrometry*, **14**, 1363–8.

Lazareth, C. E., Vander Putten, E., André, L., and Dehairs, F., 2003, High-resolution trace element profiles in shells of the mangrove bivalve *Isognomon ephippium*: a record of environmental spatio-temporal variations? *Estuarine, Coastal and Shelf Science*, **57**, 1103–14.

Le Maitre, R. W., Streckeisen, A., Zanettin, B., Le Bas, M. J., Bonin, B., Bateman, P., Bellieni, G., Dudek, A., Efremova, S., Keller, J., Lameyre, J., Sabine, P. A., Schmid, R., Sorensen, H., and Woolley, A. R., 2005, *Igneous rocks: a classification and glossary of terms. Recommendations of the International Union of Geological Sciences Subcommission on the Systematics of Igneous Rocks*, 2nd edn, 33–6, Cambridge University Press, Cambridge.

López Austin, A., and López Luján, L., 2009, *Monte Sagrado-Templo Mayor: el cerro y la pirámide en la tradición religiosa mesoamericana*, UNAM/INAH, Mexico.

López Luján, L., 1993, *Las ofrendas del Templo Mayor de Tenochtitlan*, INAH, Mexico.

López Luján, L., 2006, *La Casa de las Águilas. Un ejemplo de la arquitectura religiosa de Tenochtitlan*, 2 vols, Harvard University/FCE/INAH, Mexico.

López Luján, L., Torres, J., and Montúfar, A., 2003, Los materiales constructivos del Templo Mayor de Tenochtitlan, *Estudios de Cultura Náhuatl*, **34**, 137–66.

Matos Moctezuma, E., 1981, *Una visita al Templo Mayor*, INAH, Mexico.

Matrícula de Tributos, 1991, Secretaría de Hacienda y Crédito Público, Mexico.

Meir, I. A., Freidin, C., and Gilead, I., 2005, Analysis of Byzantine mortars from the Negev Desert, Israel, and subsequent environmental and economic implications, *Journal of Archaeological Science*, **32**, 767–73.

Miriello, D., and Crisci, G. M., 2006, Image analysis and flatbed scanners: a visual procedure in order to study the macro-porosity of the archaeological and historical mortars, *Journal of Cultural Heritage*, **7**, 186–92.

Miriello, D., Bloise, A., Crisci, G. M., Apollaro, C., and La Marca, A., 2011, Characterisation of archaeological mortars and plasters from Kyme (Turkey), *Journal of Archaeological Science*, **38**, 794–804.

Miriello, D., Bloise, A., Crisci, G. M., Barrese, E., and Apollaro, C., 2010a, Effect of milling: a possible factor influencing the durability of historical mortars, *Archaeometry*, **52**, 668–79.

Miriello, D., Bloise, A., De Francesco, A. M., Crisci, G. M., Chiaravalloti, F., Barca, D., La Russa, M. F., and Marasco, E., 2010b, Colour and composition of nodules from the Calabrian clay deposits: a possible raw material for pigments production in Magna Graecia, *Periodico di Mineralogia*, **79** (special issue), 59–69.

Miriello, D., Barca, D., Bloise, A., Ciarallo, A., Crisci, G. M., De Rose, T., Gattuso, C., Gazineo, F., and La Russa, M. F., 2010c, Characterisation of archaeological mortars from Pompeii (Campania, Italy) and identification of construction phases by compositional data analysis, *Journal of Archaeological Science*, **37**, 2207–23.

Moropoulou, A., Bakolas, A., and Aggelakopoulou, E., 2004, Evaluation of pozzolanic activity of natural and artificial pozzolans by thermal analysis, *Thermochimica Acta*, **420**, 35–140.

Moropoulou, A., Bakolas, A., and Bisbikou, K., 2000, Investigation of the technology of historic mortars, *Journal of Cultural Heritage*, **1**, 45–58.

Moropoulou, A., Polikreti, K., Bakolas, A., and Michailidis, P., 2003, Correlation of physicochemical and mechanical properties of historical mortars and classification by multivariate statistics, *Cement and Concrete Research*, **33**, 891–8.

Nicholson, H. B., 1987, Symposium on the Aztec Templo Mayor: discussion, in *The Aztec Templo Mayor* (ed. E. H. Boone), 463–80, Dumbarton Oaks, Washington, DC.

Pearce, N. J. G., Perkins, W. T., Westgate, J. A., Gorton, M. P., Jackson, S. E., Neal, C. R., and Chenery, S. P., 1997, A compilation of new and published major and trace element data for NIST SRM 610 and NIST SRM 612 glass reference materials, *Geostandards Newsletter: The Journal of Geostandards and Geoanalysis*, **21**, 115–44.

Ruffolo, S. A., La Russa, M. F., Barca, D., Casoli, A., Comite, V., Nava, G., Crisci, G. M., De Francesco, A. M., and Miriello, D., 2010, Mineralogical, petrographic and chemical analyses for the study of the canvas 'Cristo alla Colonna' from Cosenza, Italy: a case study, *Periodico di Mineralogia*, **79** (special issue), 71–9.

Sahagún, B. de, 1979, *Códice Florentino*, three vols, Secretaría de Gobernación, Mexico.

Sahagún, B. de, 2000, *Historia general de las cosas de Nueva España*, **three** vols, Conaculta, Mexico.

Scarpelli, R., De Francesco, A. M., Perri, F., Osanna, M., Colangelo, L., Miriello, D., La Russa, M. F., Barca, D., and Crisci, G. M., 2010, Archaeometric study of sub-geometric pottery found in Potenza, Italy: relationship and trade between near indigenous centers, *Periodico di Mineralogia*, **79** (special issue), 81–94.

Sinclair, D. J., 2005, Non-river flood barium signals in the skeletons of corals from coastal Queensland, Australia, *Earth and Planetary Science Letters*, **237**, 354–69.

Taylor, H. F. W., 1997, *Cement chemistry*, 2nd edn, Thomas Telford, London.

Umberger, E., 1987, Events commemorated by date plaques at the Templo Mayor: further thoughts on the solar metaphor, *The Aztec Templo Mayor* (ed. E. H. Boone), 411–50, Dumbarton Oaks, Washington, DC.

Ubbríaco, P., and Tasselli, F., 1998, A study of the hydration of lime–pozzolan binders, *Journal of Thermal Analysis*, **52**, 1047–54.

Vendrell-Saz, M., Alarcóv, S., Molera, J., and García-Vallés, M., 1996, Dating ancient lime mortars by geochemical and mineralogical analysis, *Archaeometry*, **38**, 143–9.

Wentworth, C. K., 1922, A scale of grade and class terms for clastic sediments, *Journal of Geology*, **30**, 377–92.

Wyndham, T., McCulloch, M., Fallon, S., and Alibert, C., 2004, High-resolution coral records of rare earth elements in coastal seawater: biogeochemical cycling and a new environmental proxy, *Geochimica et Cosmochimica Acta*, **68**, 2067–80.